SPECTROSCOPIC AND ION PROBE CHARACTERIZATION OF THE TRANSPORT PROCESS FOLLOWING LASER ABLATION OF $YBa_2Cu_3O_x$

DAVID B. GEOHEGAN AND DOUGLAS N. MASHBURN
Solid State Division, Oak Ridge National Laboratory, P. O. Box 2008,
Oak Ridge, TN 37831-6056

ABSTRACT

Spatial and temporal measurements of the optical absorption, optical emission and ion probe response in the ablation plume formed following pulsed 248 nm irradiation of $Y_1Ba_2Cu_3O_x$ are reported over laser energy densities from near threshold into the film growth regime. Time of flight absorbance-velocity profiles in vacuum indicate the formation and acceleration of a plasma front, with ions leading neutrals on the edge of the expanding plume. Ion probe screening measurements show that the laser plume is a well-shielded plasma with Debye lengths <10 μm at film deposition distances. Velocity distributions and estimates of ground state Ba^+, Ba, Y^+, and Y densities indicate that the populations of the ions outnumber those of the neutrals at high energy densities in vacuum. Measurements of the slowing of the plasma front and attenuation of the total charge reaching the substrate are reported for laser ablation in background pressures of oxygen. Absorption by ground state YO and BaO in the region close to the pellet indicates oxide densities $\sim 5 \times 10^{13}$ cm^{-3} close to the pellet.

INTRODUCTION

The ablation of metal oxide superconductors with high power, pulsed-excimer lasers for film growth occurs in a regime with many unknowns which can affect the quality of thin films deposited from the plume of ablated material. The fundamentals of the laser-surface interaction, the identity of the ejected species and possible photolytic reactions in the gas phase, the fractional ionization of the plume, the formation of the velocity profiles of the various species and a shock front, the interaction of the plume with background gases and the effects of the resulting kinetic energy, charge density and overall flux on the growing film are currently under investigation by a number of techniques.

Under typical film growth conditions, a high density, well-screened laser plasma is produced, usually in a background gas where collisions are important. In situ diagnostics in the film growth regime require plasma diagnostics which can operate in such an environment.

Optical emission spectroscopy can effectively study the formation and decay of excited species in the laser plume, but only indirectly views the density of ground state ion or neutral species via plasma population kinetics [1–3]. Optical absorption spectroscopy investigates instead the nonemitting ground state populations of atoms, ions, and molecules, whether moving or stopped, and has good sensitivity from the near-threshold regime into the film growth regime [4–6]. Ion probes measure the total flux and time-of-flight velocities of charged species with little selectivity, and over a wide range of plasma densities.[6–12]

In this paper, some characteristics of the $Y_1Ba_2Cu_3O_x$ ablation process, subsequent kinetics and effects of background gas pressure relevant to superconductor thin film growth are investigated with a combination of optical absorption, emission and ion probe measurements.

Mat. Res. Soc. Symp. Proc. Vol. 191. ©1990 Materials Research Society

EXPERIMENTAL

The experimental apparatus is shown in Fig. 1 and consists of a stainless steel, turbopumped bell jar in which 1-in. diam targets are rotated at 10 rpm by an externally mounted synchronous motor. The majority of the apparatus has been described previously [4,5]. An excimer laser operating at 248 nm provided 43ns FWHM pulses of up to 1 J. The beam was apertured by a vertical slit of typically 4–5 mm in width, and focused by a single cylindrical lens onto the pellet at a 60° incident angle, providing a line image of 0.8–1.0 cm length on the target surface. Quartz plates were placed between the laser and aperture to provide attenuation of the beam when necessary, and the energy of the beam was monitored on a shot-to-shot basis with a beamsplitter/pyroelectric detector (Gentec ED-200) which was calibrated to the energy delivered into the chamber.

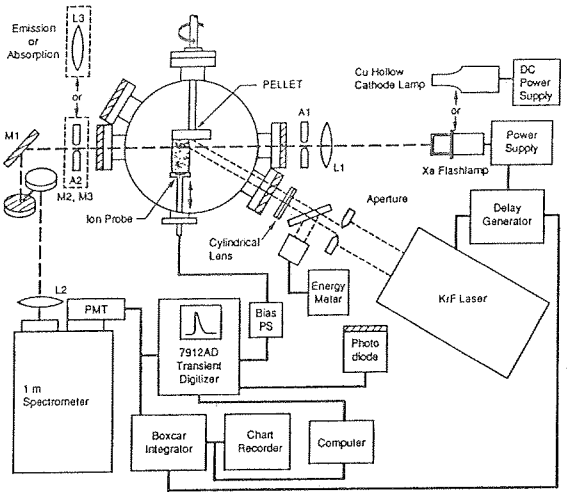

Figure 1: Schematic diagram of the experimental apparatus used for diagnostics of the laser ablation transport process. Optical absorption and emission are used to spatially and temporally characterize the populations of ground state and excited species in the plume. Ion probes are used for measurements of the velocity and flux of the expanding plasma front.

The line focus beam geometry was chosen to provide a plume which expanded little along the long dimension of the line, providing a nearly uniform 1 cm plume width up to several cm from the target. The fluorescence from the highly forward-directed laser-plasma plume was imaged onto the entrance slits of a 1-m spectrometer and was detected by a photomultiplier with 0.3 ns time response. The 0.04 Å resolution of the spectrometer provided observations of spectral broadening of atomic lines in the plume.

Optical absorption was detected by the same spectrometer/photomultiplier system in conjunction with a pulsed Xe flashlamp, which provided a structured continuum spectrum for wide spectral coverage and spectral scans. The lamp beam width was 0.5 mm across the width of the pellet. A digital delay generator controlled the time delay between the laser and boxcar averager gate (typically 50 ns width) which was set on the peak of the lamp pulse. Alternatively, a CW copper hollow cathode lamp was used to detect atomic Cu in the plume in conjunction with a second photomultiplier with interference filter. Using this arrangement, the temporal absorption of Cu on a single shot basis was recorded on a transient digitizer.

Several ion probes were utilized to monitor the total ion flux along the target normal [12]. The time response of the probes was measured to be < 3 ns. The probe used for the majority of the measurements was a flat Cu plane housed 2 mm behind a grounded Cu plane with 0.125 cm^2 aperture, onto which different meshes could be attached. The ion probe bias power supply used for time-resolved measurements was a completely isolated and shielded 1 mfd-capacitor-bypassed 60V battery and potentiometer in series with the 50 ohm signal line.

RESULTS AND DISCUSSION

The absorption of ground state ions and neutrals was studied at several distances from the pellet. Ground state neutrals and ions are detected by absorption at much lower energy densities than those required to produce visible emission at a given distance. For resonance lines with strong oscillator strengths the technique is very sensitive, allowing for densities of ~10^9 cm^{-3} to be observed over path lengths of 1 cm.[6]

At energy densities near threshold, the velocity profiles can be adequately fit by Maxwell-Boltzmann free-expansion distributions of the form,

$$\text{signal} \propto v^3 \exp\left[-m\,(v-v_{cm})^2/kT\right] \quad (1)$$

where v_{cm} is the center of mass velocity of the pulse and $v = d/\Delta\tau$ is the measured lab-frame TOF velocity.[13] Absolute number densities can also be estimated from the measured absorbance, providing that the spectral width of the absorption line is measured at the time of interest.

At higher energy densities, where plasma formation and excited state fluorescence are observed, the measured TOF absorbance profiles display several changes. Figure 2 shows the measured absorbance of both Ba and Ba^+ ground state species, 1 cm from a $Y_1Ba_2Cu_3O_x$ pellet at 10^{-5} Torr following KrF irradiation at four energy densities. Although the spectral broadening changes somewhat throughout the higher energy density scans, making the absorbance no longer directly analogous to density, several key features are displayed.

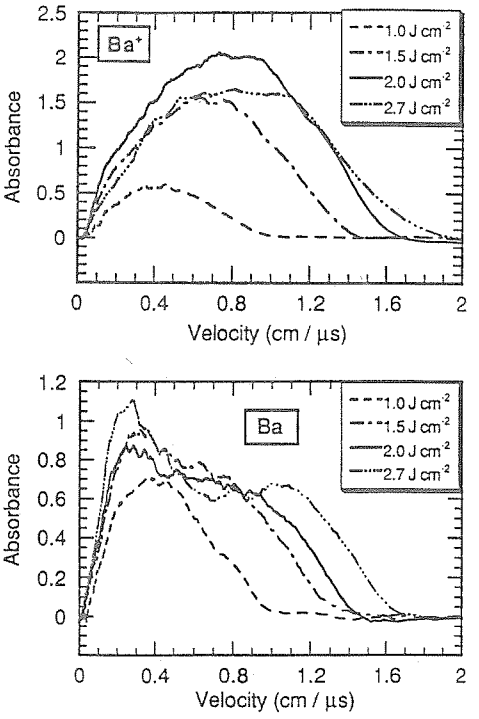

Figure 2: Measured absorbances vs time-of-flight velocity for ground state Ba (553.5 nm) and Ba^+ (445.4 nm) at d = 1 cm from a $Y_1Ba_2Cu_3O_x$ pellet at 10^{-5} Torr following KrF irradiation at four energy densities.

First, up to 1.0 J cm^{-2} the profiles for Ba^+ and Ba are very similar in magnitude, shape and leading edge velocity. Spectral widths measured at the peak of the 1.0 J cm^{-2} absorbances, however, imply that Ba^+ ions outnumber Ba neutrals by 5 to 1.

At the higher energy densities, the ions grow more rapidly in number, and appear on the leading edge of the expanding plume, with the neutrals lagging behind. In addition, the neutral distribution takes on a two-component appearance with a fast component trailing the ion fast component, and a slow component. Fluorescence from excited Ba^* (not shown) mimics the fast component of the neutral profile and is gone approximately at the peak of the ground state neutral absorbance.[6,8] Similarly, fluorescence from $(Ba^+)^*$ was also observed between the leading edge of the ion pulse and the peak of the ground state ion absorbance.

These measurements show that the Ba in the plume is highly ionized in vacuum and that at least a portion of the fast component of the neutral pulse can be attributed to recombination of ions on the leading edge of the pulse, supported by the recombination-fed fluorescence. The existence of $(Ba^+)^*$ fluorescence preceding the ground state Ba^+ absorption also suggests the existence of Ba^{++} ahead of the Ba^+ absorption. Similar results were obtained for Y and Y^+.

Estimates of the overall fractional ionization of the plume were made by comparing the mass of collected material and the integrated positive charge arriving through an aperture on an ion probe at d=5 cm following 3.3 J cm^{-2} KrF irradiation of a $Y_1Ba_2Cu_3O_x$ pellet in vacuum. The results indicated that ~25% of the plume was ionized (assuming singly ionized species and neglecting etching of the film by the high ion energies) at this high energy density.

In order to trace the increase in ionization and acceleration of the plasma front with increasing energy density, a series of ion probe waveforms were digitized at a fixed distance of 2.9 cm in vacuum. The variation of total collected positive charge with KrF laser energy density is given in Fig. 3. The measurements range from the near-threshold region where only a faint fluorescent mark was visible on the pellet surface to the high ionization conditions described

above. The data display two main regimes. Below 0.32 J cm^{-2}, circa ablation threshold, the total charge reaching the probe varies sharply as I^8, where I is the laser intensity. Above 0.7 J cm^{-2}, the charge increases as $I^{1.6}$.

The velocities of the ions were also simultaneously measured by recording the arrival times of the peak and the leading edge (10% of the peak) of the ion flux signal from the ion probe. The results are given in Fig. 4 and show that the ion velocity increases more rapidly at lower energy densities. The absorbance data of Fig. 2 for Ba^+ displayed the same general saturation dependence on energy density, following the curves of Fig. 4.

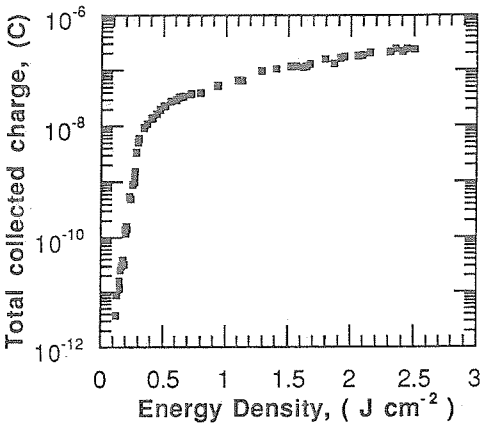

Figure 3: Total charge collected 2.9 cm along the normal from a $Y_1Ba_2Cu_3O_X$ pellet through a 0.125 cm^2 aperture at 10^{-5} Torr with a Cu planar ion probe. The probe was biased at -30.7 V.

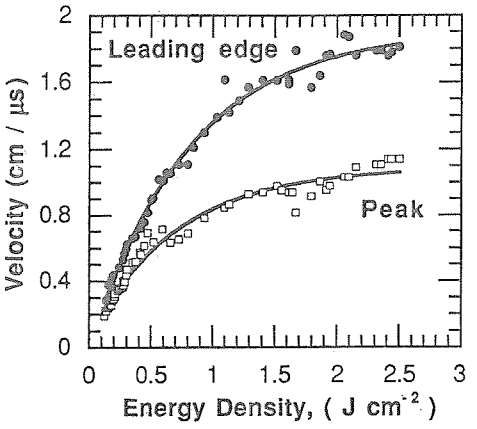

Figure 4: TOF velocity of the expanding plasma front, 2.9 cm along the normal from a $Y_1Ba_2Cu_3O_X$ pellet in vacuum, as measured with an ion probe. Two time intervals were obtained from digitized waveforms, corresponding to the peak and the leading edge (defined as 10% of the peak) ion flux.

To explain the increase in velocity of the ions with increasing laser intensity, the interaction of the laser with the expanding plasma [14,15] during the laser pulse has been proposed. In the model, the plasma electrons are heated by the inverse Bremmstrahlung process and accelerate the ions electrostatically after nearly escaping the ion field. The electrons are drawn back and thermalized in collisions with the ions and then repeat the process many times throughout the laser pulse.

The data of Figs. 3 and 4 support a laser interaction with the plasma as a means of ion acceleration. The coincidence in energy density between the knee in Fig. 3 and visible plasma emission indicates a change in the laser-target interaction during plasma formation. The increase in plasma absorption allows less of the laser pulse to reach the surface of the pellet, resulting in a limiting of the near-threshold ionization process.

The interaction of the laser light and plasma with ejected clusters has been shown to fragment the clusters into smaller oxides and monatomics [16] and has been suspected as the origin of a slower component to the transport process [17].

Close to the pellet, within the bright plasma, strong absorption by the diatomic oxides has been measured. Figure 5 gives an absorption spectrum of YO ($A^2\Pi_{3/2} \leftarrow X$) at a distance of 2 mm from a $Y_1Ba_2Cu_3O_X$ pellet

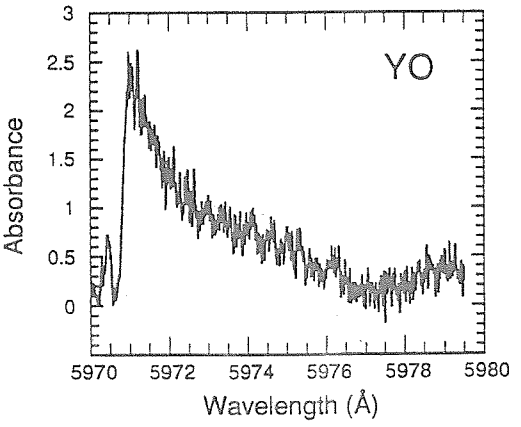

Figure 5: The absorption spectrum of YO (A←X) indicating a YO density of ~5×10^{13} cm^{-3} at d=2 mm from a $Y_1Ba_2Cu_3O_X$ pellet following 1.5 J cm^{-2} KrF irradiation.

following 1.5 J cm^{-2} irradiation at 248 nm. From measured transition moments for this band [18], YO densities of ~5 ¥ 10^{13} cm^{-3} can be estimated. Similar strong absorption was noted for BaO.

When laser ablation takes place in the presence of a background gas, collisions between the plasma plume and the gas limit the distance and velocity that the deposition products may travel. To investigate the dropoff of positive ion flux and arrival velocity at a substrate under deposition conditions, an ion probe (aperture 0.125 cm^2, bias -57 V) was positioned at various distances along the normal to the irradiated region on the pellet following 3 J cm^{-2} KrF irradiation in several oxygen backpressures. The total positive charge collected by the probe and the velocity of the leading edge of the plasma front were measured from the digitized ion probe signals and are given in Figs. 6 and 7, respectively.

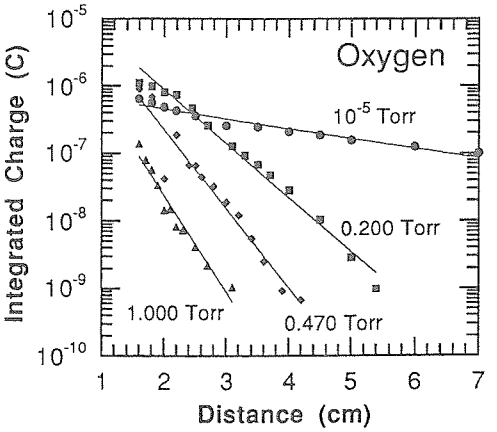

Figure 6: Attenuation of collected positive charge with distance along the $Y_1Ba_2Cu_3O_x$ pellet normal in background oxygen pressures of 10^{-5}, 0.200, 0.470, and 1.000 Torr following 3 J cm^{-2} KrF irradiation. Probe area 0.125 cm^2, bias -57 V.

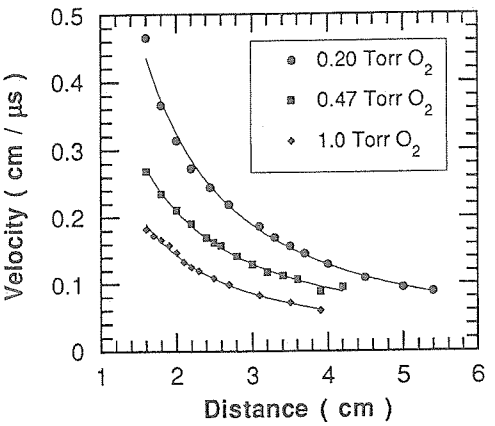

Figure 7: Slowing of the expanding plasma front (10% ion flux peak) with distance along the $Y_1Ba_2Cu_3O_x$ pellet normal due to background oxygen pressures of 0.200, 0.470, and 1.000 Torr following 3 J cm^{-2} KrF irradiation.

With 10^{-5} Torr of background oxygen, the leading edge of the plasma front maintained a constant velocity of 2.0 cm μs^{-1} from d = 1.6 cm (minimum probe distance) to d > 20 cm while the total collected positive charge was found to decrease as $d^{-1.25}$. At higher oxygen pressures the total collected charge decreased roughly exponentially with distance, as indicated by the exponential best-fits to the data in Fig. 6. While the data likely reflect a combination of complicated kinetic processes (such as the combined effects of scattering, species-specific ion production and recombination, velocity-dependent collision cross-sections, etc.) the data of Figure 6 gives an indication of the overall charge deposition experienced by a substrate immersed in the plume. Measurements of the attenuation of Cu neutrals by background oxygen and argon using the hollow cathode lamp indicated similar attenuation dependences and ranges for Cu neutrals, indicating that the ion probe provides a measure of the useful range and rate over which film deposition can take place at a given laser power and background gas pressure.

The arrival velocity of the ions in the plume is given in Fig. 7 at three background oxygen pressures. The velocities in Fig. 7 are not simple TOF velocities, but were obtained by calculating the slope of the distance vs arrival time data. Without collisional slowing by the oxygen, Ba^+ velocities of 2.0 cm μs^{-1} were measured on the leading edge of the plume, corresponding to kinetic energies of ~ 290 eV. The ion probe measurements of Fig. 7 provide an upper limit to the ion energies in the plume at a given distance and background pressure. For example, at d = 3.0 cm, Ba^+ maximum energies of ~ 2.6 eV, 1.2 eV and 0.53 eV are estimated for background oxygen pressures of 0.20 Torr, 0.47 Torr and 1.0 Torr, respectively.

The combination of localized ion flux and kinetic energy estimates provided by ion probes in the plasma plume provide a powerful and necessary diagnostic to gauge the substrate environment for different choices of deposition conditions. Ion probe and optical deposition

monitors should facilitate the search for equivalent deposition conditions over a wide range of possible experimental parameters.

SUMMARY

Optical absorption spectroscopy and ion probe measurements have been applied to investigate the plume produced by 248 nm irradiation of $Y_1Ba_2Cu_3O_x$ under film growth conditions. The plume is characterized as a partly ionized plasma with some of the monatomic species predominantly singly ionized at the higher laser energy densities. Increasing laser energy density at the target results in acceleration of the plasma boundary in which the ions precede the neutrals with evidence of recombinational feeding of the ground state neutral population. Laser interaction with the plasma plume is indicated by the change in ion production rate with the onset of visible plasma fluorescence. The variations of the velocity of the plasma front and of the total positive charge delivered to the substrate, with energy density and background oxygen pressure have also been measured.

ACKNOWLEDGEMENTS

The authors gratefully acknowledge the technical assistance of G. E. Jellison, Jr., H. A. Harmon, B. C. Sales, D. H. Lowndes, and D. P. Norton. Research sponsored by the Division of Materials Sciences, U. S. Department of Energy under contract DE-AC05-84OR21400 with Martin Marietta Energy Systems, Inc.

REFERENCES

1. J. P. Zheng, Q. Y. Ying, S. Witanachchi, Z. Q. Huang, D. T. Shaw, and H. S. Kwok, *Appl. Phys. Lett.* **54**, 954 (1989).
2. K. L. Saenger, *J. Appl. Phys.* **66**, 4435 (1989).
3. C. Girault, D. Damiani, J. Aubreton, and A. Catherinot, *Appl. Phys. Lett.* **55**, 182 (1989).
4. D. B. Geohegan and D. N. Mashburn, *Appl. Phys. Lett.* **55**, 2345 (1989).
5. D. B. Geohegan and D. N. Mashburn, Third Annual Conference on Superconductivity and Applications, Plenum Press, New York (in press).
6. A. D. Akhsakhalyan, Yu A. Bityurin, S. V. Gaponov, A. A. Gudkov, and V. I. Luchin, *Sov. Phys. Tech. Phys.* **27**, 969 (1982).
7. W. Demtröder and W. Jantz, *Plasma Physics* **12**, 691 (1970).
8. R. J. von Gutfeld and R. W. Dreyfus, *Appl. Phys. Lett.* **54**, 1212 (1989).
9. S. K. Goel, P. D. Gupta, and D. D. Bhawalkar, *J. Appl. Phys.* **53**, 2971 (1982).
10. P. E. Dyer, *Appl. Phys. Lett.* **55**, 1630 (1989).
11. P. E. Dyer, R. D. Greenough, A. Issa, and P .H. Key, *Appl. Phys. Lett.* **53**, 534 (1988).
12. D. N. Mashburn and D. B. Geohegan, in *Symposium on Microelectronic Integrated Processing: Growth, Monitoring, and Control,* The Society for Photo-Optical Engineers (SPIE), Bellingham, Washington (in press).
13. Roger Kelly and R. W. Dreyfus, *Surf. Sci.* **198**, 263 (1988).
14. Yu A. Bykovskii, N. N. Degtyarenko, V. F. Elesin, V. E. Kondrashov, and E. E. Lovetskii, *Sov. Phys. Tech. Phys.* **18**, 1597 (1974).
15. H. Puell, Z. *Naturforsch.* **25a**, 1807 (1970).
16. C. H. Becker and J. B. Pallix, *J. Appl. Phys.* **64**, 5152 (1988).
17. O. Eryu, K. Murakami, and K. Masuda, *Appl. Phys. Lett.* **54**, 2716 (1989).
18. K. Liu and J. M. Parson, *J. Chem. Phys.* **67**, 1814 (1977).